Journal of Information Display
Vol. 13, No. 2, June 2012, 91–95

Taylor & Francis
Taylor & Francis Group

InP/ZnSe/ZnS: A Novel Multishell System for InP Quantum Dots for Improved Luminescence Efficiency and Its application in a Light-Emitting Device

Christian Ippen, Tonino Greco and Armin Wedel*

Functional Materials and Devices, Fraunhofer Institute for Applied Polymer Research, Potsdam 14476, Germany

(*Received 30 December 2011; Revised 28 February 2012; Accepted for publication 06 March 2012*)

Indium phosphide (InP) quantum dots (QDs) are considered alternatives to Cd-containing QDs for application in light-emitting devices. The multishell coating with ZnSe/ZnS was shown to improve the photoluminescence quantum yield (QY) of InP QDs more strongly than the conventional ZnS shell coating. Structural proof for this system was provided by X-ray diffraction and transmission electron microscopy. QY values in the range of 50–70% along with peak widths of 45–50 nm can be routinely achieved, making the optical performance of InP/ZnSe/ZnS QDs comparable to that of Cd-based QDs. The fabrication of a working electroluminescent light-emitting device employing the reported material demonstrated the feasibility of the desired application.

Keywords: indium phosphide; multishell; colloidal quantum dots; QLED

Introduction

Semiconductor quantum dots (QDs) show fascinating optical properties, such as size-tunable emission color, narrow emission peak, and high luminescence efficiency. These properties can be utilized advantageously in quantum dot light emitting devices (QLEDs) and solar cells, and for bio-imaging purposes [1]. Additionally, colloidal QDs can be processed using cost-effective solution-based methods like spin coating or contact printing [2].

Most of the past researches on colloidal QDs focused on cadmium chalcogenide materials such as CdSe and CdS, which can be synthesized in high quality through a simple and reliable procedure [3]. The toxicity of cadmium materials, however, and the corresponding regulation exclude any real-world application of cadmium-based QDs and hence necessitate a search for alternatives. For the emission of visible light, indium phosphide (InP) is considered the most promising alternative [4]. Up to now, however, the reported optical properties of InP are inferior to those of CdSe, especially with regard to the photoluminescence quantum yield (QY) and peak width [5].

Typically, QDs are coated with another semiconductor material with a wider bandgap to yield a shell that passivates surface defects and thus improves the luminescence efficiency [6]. An important criterion for the selection of the shell material is the similarity of the lattice constants of the core and the shell material, which should not differ by more than 12% to allow for the epitaxial growth of the shell [7]. Often, zinc sulfide is the material of choice for passivating both CdSe and InP QDs, although it has a considerable lattice mismatch to both. The shell coating can be improved by using intermediate shell layers with better-fitting lattice constants, which reduce interfacial stress. Concerning CdSe QDs, multishell coatings such as CdSe/CdS/ZnS and CdSe/ZnSe/ZnS have been shown to be advantageous in terms of photoluminescence QY and stability [8,9].

Here, a method of improving the luminescence efficiency of InP QDs by coating with a ZnSe/ZnS multishell, which provides higher QY improvements compared with ZnS monoshell coating, is reported. The use of such method results in a cadmium-free QD material with an optical performance comparable to that of cadmium-based QDs. The InP/ZnSe/ZnS QD material was also successfully employed in a QLED, demonstrating the feasibility of this application.

Experiment

Materials and methods

All the chemicals were purchased from Sigma-Aldrich or Alfa Aesar, and were used without further purification. All the reactions were carried out under inert conditions, by means of the Schlenk technique. UV–VIS spectra were acquired using a PerkinElmer Lambda 19 spectrometer. Photoluminescence spectroscopy and QY determination were carried out using a Hamamatsu C9920-02 system, based on an integrating sphere. X-ray diffraction (XRD) was performed on a Bruker D8 advance instrument.

*Corresponding author. Email: armin.wedel@iap.fraunhofer.de

ISSN 1598-0316 print/ISSN 2158-1606 online

http://dx.doi.org/10.1080/15980316.2011.683537
http://www.tandfonline.com

Transmission electron microscopic (TEM) images were taken using a Phillips CM 200 instrument. Electroluminescence spectra were acquired with a Konica-Minolta CS-2000 spectroradiometer. The light-emitting devices were driven by a Keithley SMU 236.

Synthesis procedures

The InP core nanoparticles were synthesized using a slightly modified version of the heating-up procedure developed by Li and Reiss [10]. In brief, indium myristate (0.1 mmol, 1 mL of a 0.1 M stock solution), zinc stearate (0.1 mmol, 63 mg), dodecanethiol (0.05 mmol, 12 μL), and tris(trimethylsilyl) phosphine (0.1 mmol, 100 μL of a 1 M stock solution) were dissolved in octadecene and were subsequently heated to 300°C for 3 min. The reaction was maintained at 300°C for 30 min and was monitored via photoluminescence spectroscopy on aliquots taken at different time intervals. The raw solution of the InP core nanoparticles was used for shell synthesis, without purification.

For the synthesis of a ZnS monoshell, zinc stearate (0.4 mmol, 253 mg) and cyclohexyl isothiocyanate (0.2 mmol, 200 μL of a 1 M stock solution) were added to a raw solution of InP nanoparticles (0.1 mmol In). The mixture was then heated to 280°C for 20 min.

For the multishell system, first, zinc stearate (0.1 mmol, 63 mg) and trioctylphosphine selenide (0.05 mmol, 50 μL of a 1 M stock solution) were added to a raw solution of InP nanoparticles (0.1 mmol In). The mixture was then heated to 280°C for 20 min to produce a ZnSe shell. Subsequently, zinc stearate (0.3 mmol, 189 mg) and cyclohexyl isothiocyanate (0.15 mmol, 150 μL of a 1 M stock solution) were added to a raw solution of InP/ZnSe nanoparticles. The mixture was then heated to 280°C for 20 min to yield a ZnS shell.

The resulting core-shell nanoparticles were purified through repeated precipitation and centrifugation, using a toluene/ethanol solvent mixture for further characterization and device fabrication.

Device preparation

ITO-coated (indium tin oxide) silica glass substrates were cleaned in an ultrasonic bath before use. PEDOT:PSS (poly(3,4-ethylenedioxythiophene):poly(styrenesulfonate) was spin-coated as a hole injection layer on top of the ITO layer. TPD polymer (Poly[N,N′-bis(4-butylphenyl)-N,N′-bis(phenyl)-benzidine]) was spin-coated from a chlorobenzene solution. The QDs were dispersed in toluene and were spin-coated onto the TPD layer. Thin films of TBPI (2,2′,2″-(1,3,5-benzinetriyl)-tris(1-phenyl-1-H-benzimidazole), barium, and aluminium were consecutively deposited via thermal evaporation. The device structure was encapsulated with a cover glass fixed with low-permeation epoxy resin. All the sample preparation steps were carried out under an inert nitrogen atmosphere in glove box systems situated in a clean room.

Results and discussion

Optical properties

The InP core QDs were obtained through the heating-up procedure reported by Li and Reiss [10], where zinc and sulfur precursors were already added to the core synthesis, which inhibits the particle ripening and, thus, accounts for the narrow size distribution shown by the emission peak widths in the range of 45–50° nm. This can be attributed to the formation of a thin ZnS shell [10], the formation of InPZnS alloy with different growth properties [11], or only to the adsorption of the zinc and sulfur precursors to the particle surface. This matter has not been resolved and will not be further discussed in this paper.

Monoshell passivation with ZnS was carried out through a procedure similar to that reported by Ziegler *et al*. [12], using cyclohexyl isothiocyanate as a sulfur precursor. On average, an improvement in the photoluminescence QY by a factor of 2 was observed with the monoshell coating.

The ZnSe/ZnS coating leads to a strong increase in luminescence efficiency, which is visualized by the photograph of the InP, InP/ZnSe, and InP/ZnSe/ZnS samples shown under UV illumination in Figure 1. The absorption and photoluminescence spectra are shown in Figure 2. A slight (about 20 nm) red shift can be seen on the multishell coating. The peak width remained unchanged at about 45 nm full-width at half-maximum for both shell-coating steps.

The multishell synthesis method showed good reproducibility. Based on 28 experiments on different InP batches, an average QY improvement of a factor of 4.1 after both shell synthesis steps was observed. The average red shift was 16 nm and is attributed to the weaker confinement provided by the ZnSe intermediate shell because of its lower bandgap compared with ZnS.

The absolute QY values also depend on the quality of the core InP particles, which probably originates from the crystal defects within the core particles contributing to the non-radiative recombination. Routinely, QY values in the range of 50–70% are achieved.

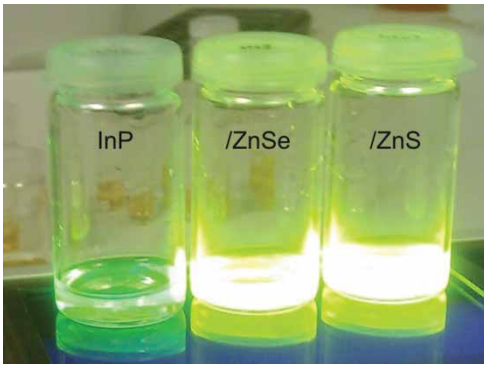

Figure 1. InP, InP/ZnSe, and InP/ZnSe/ZnSQD samples (from left to right) under UV illumination, with QY values of 25%, 54%, and 59%, respectively (color online).

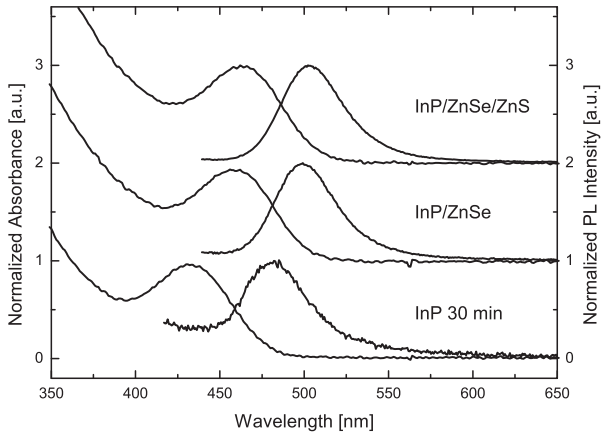

Figure 2. UV–VIS and PL spectra of the InP, InP/ZnSe, and InP/ZnSe/ZnS QD samples (corresponding to the TEM images in Figure 4).

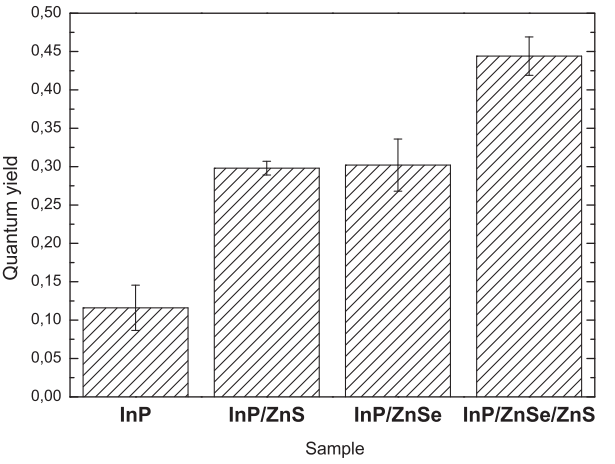

Figure 3. Direct comparison of the ZnS monoshell and the ZnSe/ZnS multishell in terms of QY. The values are arithmetic means from five experiments, and the error bars are the corresponding standard errors.

Direct comparison of the monoshell and multishell

To prove the superiority of the ZnSe/ZnS multishell over the ZnS monoshell, five InP batches were divided into two parts each. The first was then coated with ZnSe/ZnS, and the second with the ZnS shell. The use of identical InP samples for shell comparison excluded any variation resulting from the subtle changes in the InP surface chemistry. The ZnS coating was carried out in two steps, as with the multishell coating, to account for any effect resulting from the thermal cycling.

The QY values obtained from this direct comparison are shown in Figure 3. On average, the QY was about one-fourth higher for the ZnSe/ZnS multishell than for the ZnS monoshell. Improvement of the QY of the InP QDs with a ZnSe/ZnS multishell instead of a ZnS monoshell was achieved. This was most likely the result of the improved compatibility of the ZnSe layer, whose bulk lattice constant of 5.67 Å is in between those of InP (5.87 Å) and ZnS (5.41 Å). As a large difference in lattice constants leads to strain in the shell, a ZnS shell on InP is more strained and, therefore, contains more defects than a ZnSe shell on InP or a ZnS shell on ZnSe. Defects in the shell quench the photoluminescence, which explains the stronger luminescence increase with the ZnSe intermediate shell.

Structural characterization

The TEM images in Figure 4 of the samples whose spectra are shown in Figure 2 show spherical, uniform nanoparticles with increasing size for the successive shell synthesis steps. The measured particle sizes were 2.3 ± 0.3 nm for the InP core QDs, which were consistent with the particle size of 2.5 nm calculated from the exciton absorption peak at 430 nm [7]. After the ZnSe shell synthesis, the particle size increased to 2.6 ± 0.2 nm, which corresponds to the deposition of about one shell monolayer. After the final ZnS shell deposition, the particle diameter was 3.3 ± 0.3 nm, brought about by the two ZnS monolayers. The narrow size distribution of 10% confirms the narrow emission peak width values of 45–50 nm routinely obtained for this QD material.

To prove the formation of the three different phases, the samples resulting from each synthesis step (InP core, InP/ZnSe first shell, InP/ZnSe/ZnS second shell) were purified and subjected to powder XRD. The diffraction patterns for the three samples are shown in Figure 5, along with the reflection angles of the corresponding bulk materials InP (ICDD PDF 00-032-0452), ZnSe (ICDD PDF 01-071-5977), and ZnS (ICDD PDF 04-006-2561).

Due to the peak width resulting from the nanoscale size of the particles and due to the similarity of the lattices,

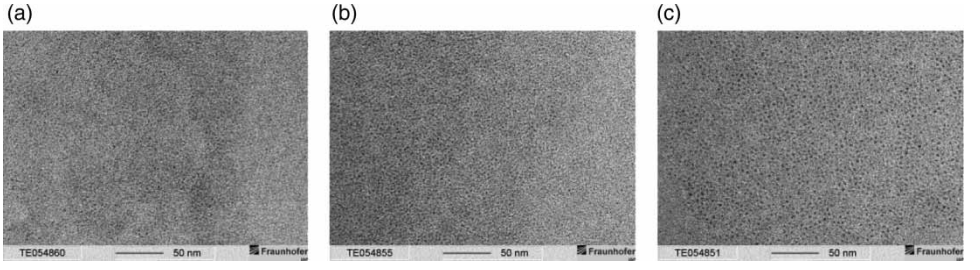

Figure 4. TEM images of the (a) InP, (b) InP/ZnSe, and (c) InP/ZnSe/ZnS QDs (corresponding to the spectra in Figure 2).

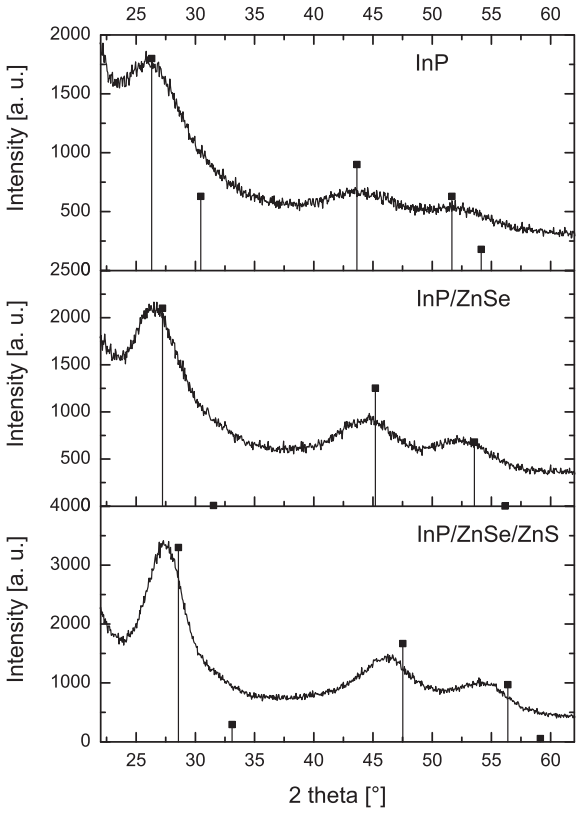

Figure 5. XRD patterns for the InP, InP/ZnSe, and InP/ZnSe/ZnS samples. The vertical lines are the reflections of the bulk InP, ZnSe, and ZnS, respectively (ICDD PDF 00-032-0452, 01-071-5977, and 04-006-2561).

the reflections of the three phases were not resolved, but a distinct shift in the reflections upon shell coating toward the expected bulk material reflection angles was observed. As the QY, which is determined by the particle surface, was strongly improved, a core-shell assembly of the different phases is more likely than an alloyed phase, which could also result in the observed diffraction pattern. Furthermore, the observed red shift of the emission wavelength confirmed the formation of a core-shell system rather than an alloy because the latter should result in a larger bandgap and, therefore, a blue shift.

Device performance

Light-emitting devices were assembled using the InP/ZnSe/ZnS QD material as a light-emitting layer in a sandwich structure, as shown in Figure 6(a). PEDOT: PSS and TPD were used as hole-transporting layers. The QD layer was spin-coated from toluene on the TPD. TPBI as electron transport layer as well as Ba and Al layers as cathode system were deposited via thermal evaporation. The corresponding energy levels and charge transport paths are depicted schematically in Figure 6(b). Figure 6(c) shows the electroluminescence spectrum of a device driven at 10 V, and the photoluminescence spectrum of the QDs dispersed in toluene prior to the device fabrication. In the QLED, there was a substantial emission contribution in the blue-wavelength range, which presumably originated from the hole-transporting material TPD. Nevertheless, the sharp QD emission is clearly identifiable, although the emission peak shifted by about 15 nm and slightly broadened compared with the photoluminescence. The device exhibited a luminance of 26 cd/m^2 at 15 V, which is a promising first result. The device performance is, therefore, similar to that recently reported by the group of Changhee Lee, who achieved a luminance of 16 cd/m^2 at 11 V with

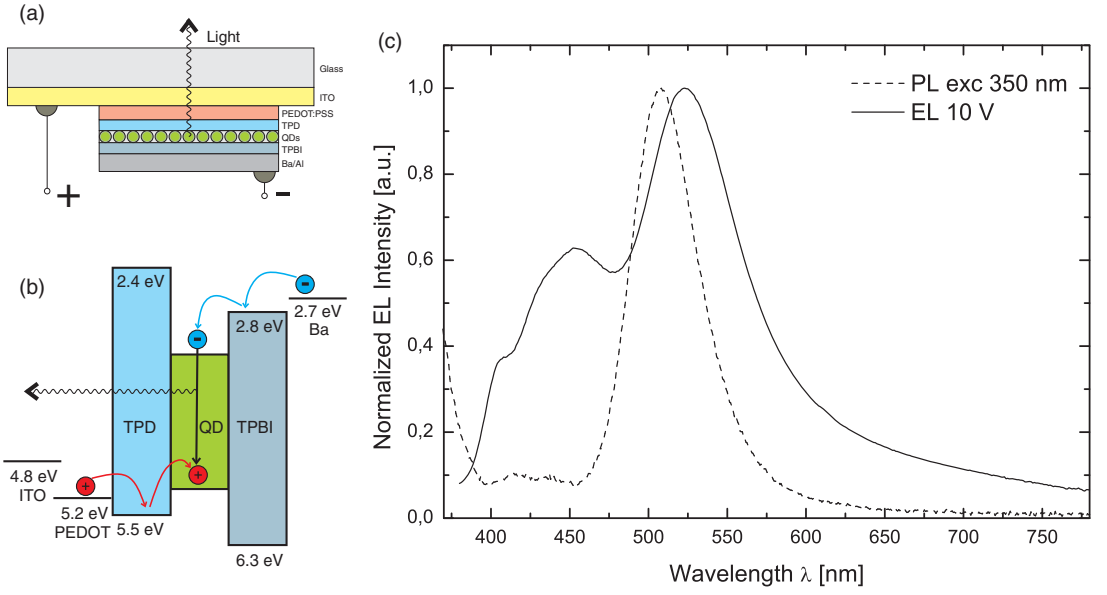

Figure 6. Electroluminescent device employing InP/ZnSe/ZnS QDs: (a) device schematics, (b) electronic structure corresponding to the device setup, and (c) solution photoluminescence and electroluminescence spectra.

a very similar QD material, namely InP with a ZnSeS shell with gradient composition [13]. It is believed that the device performance can be improved in the future experiments by optimizing the film thicknesses, the charge carrier transport materials, and the ligands on the nanoparticle surface.

Conclusion

InP/ZnSe/ZnS was introduced as a new core-shell QD material that showed improved photoluminescence QY compared with the conventional InP/ZnS system. Photoluminescence QYs in the range of 50–70% can be routinely achieved, making the performance of the InP-based QDs comparable to that of the Cd-based QDs. The fabrication of a light-emitting device (QLED) employing multishell QDs demonstrated the feasibility of the use of cadmium-free QDs in QLEDs.

Acknowledgements

The authors thank Stefanie Kreissl for the device preparation, and Stefan Glatzel for helping with the XRD and TEM measurements. This research was supported by QD-LED Project of International Cooperation Program funded by the Ministry of Knowledge and Economy, South Korea.

References

[1] D. Bera, L. Qian, T.-K. Tseng, and P.H. Holloway, Materials **3**, 2260 (2010).
[2] L. Kim, P.O. Anikeeva, S.A. Coe-Sullivan, J.S. Steckel, M.G. Bawendi, and V. Bulovicì, Nano Lett. **8**, 4513 (2008).
[3] D.V. Talapin, A.L. Rogach, A. Kornowski, M. Haase, and H. Weller, Nano Lett. **1**, 207 (2001).
[4] R. Xie, D. Battaglia, and X. Peng, J. Am. Chem. Soc. **129**, 15432 (2007).
[5] P. Mushonga, M. Onani, A.M. Madiehe, and M. Meyer, J. Nanomater. (2011). doi:10.1155/2012/869284
[6] B.O. Dabbousi, J. Rodriguez-Viejo, F.V. Mikulec, J.R. Heine, H. Mattoussi, R. Ober, K.F. Jensen, and M.G. Bawendi, J. Phys. Chem. B **101**, 9463 (1997).
[7] P. Reiss, M. Protière, and L. Li, Small **5**, 154 (2009).
[8] D.V. Talapin, I. Mekis, S. Götzinger, A. Kornowski, O. Benson, and H. Weller, J. Phys. Chem. B **108**, 18826 (2004).
[9] R. Xie, U. Kolb, J. Li, T. Basché, and A. Mews, J. Am. Chem. Soc. **127**, 7480 (2005).
[10] L. Li and P. Reiss, J. Am. Chem. Soc. **130**, 11588 (2008).
[11] K. Huang, R. Demadrille, M.G. Silly, F. Sirotti, P. Reiss, and O. Renault, ACS Nano **4**, 4799 (2010).
[12] J. Ziegler, S. Xu, E. Kucur, F. Meister, M. Batentschuk, F. Gindele, and T. Nann, Adv. Mater. **20**, 4068 (2008).
[13] J. Lim, W.K. Bae, D. Lee, M.K. Nam, J. Jung, C. Lee, K. Char, and S. Lee, Chem. Mater. **23**, 4459 (2011).